Biochimica et Biophysica Acta, 553 (1979) 262—283

BBA 78359

THYMIDINE TRANSPORT IN CULTURED MAMMALIAN CELLS

KINETIC ANALYSIS, TEMPERATURE DEPENDENCE AND SPECIFICITY OF THE TRANSPORT SYSTEM

ROBERT M. WOHLHUETER, RICHARD MARZ * and PETER G.W. PLAGEMANN

Department of Microbiology, University of Minnesota Medical School, Minneapolis, MN 55455 (U.S.A.)

(Received September 22nd, 1978)

Key words. Nucleoside transport properties, Thymidine, (Mammalian cell)

Summary

The transport of thymidine has been characterized kinetically and thermodynamically in Novikoff rat hepatoma cells grown in culture and, less extensively, in mouse L cells, Chinese hamster ovary cells, P388 murine leukemia cells and HeLa cells. That the characterizations pertained to the transport system per se was ensured, (i) by employing recently developed methods for rapid sampling of cell/substrate mixtures in order to follow isotope movements within a few seconds after initial exposure of cells to substrate; (ii) by utilizing cells rendered, by genetic or chemical means, incapable of metabolizing thymidine; and, (iii) by demonstrating conformity of the transport data to an integrated rate equation derived for a simple, carrier-mediated system. The results indicate that thymidine is transported into mammalian cells by a functionally symmetrical, non-concentrative system for which the carrier : substrate dissociation constant ranges from about 100 μM in Chinese hamster ovary cells, to 230 μM in Novikoff hepatoma cells. In all cell lines investigated, the velocity of transport was sufficient to nearly completely equilibrate low concentrations of thymidine across the membrane within 15 s. Temperature dependence of

---

Abbreviation: CHO cells, Chinese hamster ovary cells. We follow the nomenclature and symbols of Eilam and Stein [5]. 'Zero-*trans*' (designated zt in superscripts) refers to the transfer of substrate from side 1 of the membrane (= outside) to side 2 (the '*trans*' side), at which concentration of substrate is, or is assumed to be, zero. 'Equilibrium exchange' (designated ee) refers to isotopic exchange across the membrane when the chemical concentration of substrate is equal on both sides. 'Infinite-*trans*' (designated it) refers to the flux of isotope from one side of the membrane at low concentration of substrate to the '*trans*' side at saturatingly high concentration. The order of numerical subscripts indicates the direction of measured flow, e.g. 12 indicates from outside to inside.

* Present address: Institut für Molekularbiologie der Österreichischen Akademie der Wissenschaften, Billrothstr. 11, A5070 Salzburg, Austria.

transport velocity and substrate : carrier dissociation were continuous (E_A = 18.3 kcal/mol, $\Delta H^{0\prime}$ = 9.3 kcal/mol, respectively), and showed no evidence of abrupt transitions. Several natural and artificial nucleosides and nucleic acid bases inhibited influx of radiolabeled thymidine, apparently by competing with thymidine for the transport carrier.

Introduction

Mammalian cells grown in culture rapidly incorporate exogenous purine and pyrimidine nucleosides via a variety of salvage pathways. Incorporation is a complex process involving, in its simplest version, transport of the nucleosides across the cell membrane, multiple phosphorylations resulting in its entry into cellular nucleotide pools, and finally polymerization into nucleic acid. With certain nucleosides the process becomes more ramified, as phosphorolysis or deamination compete with phosphorylation. Even so, the rates of incorporation of several nucleosides into total cellular material have been observed to obey simple Michaelian kinetics, suggestive of a single, saturable, rate-determining step in the overall process.

Recently we have developed methodology which allows us to distinguish kinetically the transport step from subsequent metabolic steps [1,2]. Using rapid mixing techniques similar to those of the stop-flow kineticist, we can follow the progress of substrate permeation and intracellular metabolism at intervals as short as 1 s. Initial explorations with this methodology have made two points: (i) the kinetic behavior of the nucleoside transporters is unambiguously different from that of the nucleoside incorporation systems, and (ii) free nucleoside equilibrates rapidly (within seconds at concentrations below the K_m of transport), while the slower phosphorylation of intracellular nucleoside determines the long-term rate of incorporation [3,4].

The transport step revealed by these methods is most advantageously assayed in cells incapable of metabolizing a given nucleoside substrate, as, for example, in mutants deficient in a particular nucleoside kinase, or in cells depleted of ATP. The advantage in using a non-metabolizing system is that the entire time course of the attainment of transmembrane equilibrium (the duration of which may be less than 15 s) can be followed; the data thus obtained can be analyzed in terms of integrated rate equations to yield considerable information on the mechanism of transport.

Previously we have evaluated such time courses by means of the integrated form of a first-order rate equation, which (for reasons elaborated in Ref. 2) can only approximate initial velocities of substrate entry. Now we have developed computational procedures by which exact, integrated rate equations derived for various carrier-mediated transport models can be fit directly, without logarithmic transforms, to zero-*trans* influx data.

The combination of rapid mixing/sampling techniques with integrated rate analysis has made it technically possible to characterize nucleoside transport per se in cultured mammalian cells, without interference from metabolic events. We believe that such a characterization is also scientifically expedient, since much of the literature on the 'transport' of nucleosides and nucleic acid

bases into cultured mammalian cells is predicated on the assumption that the transport step is rate determining for the incorporation of these substances into total cellular material. This assumption is not generally true [3,4,6,7], and recent work shows that it may be the exception, rather than the rule.

We have taken this combined approach to a kinetic analysis of thymidine transport in five cell lines. For one of these cell lines, Novikoff rat hepatoma, we have extended the kinetic studies to include also isotopic exchange across the cell membrane and the temperature dependence of both influx and exchange reactions. Furthermore, we present evidence for an apparently broad specificity of the thymidine transporter, based on the inhibition of influx of radiolabeled thymidine in the presence of various, non-labeled nucleosides and nucleic acid bases.

Materials and Methods

Cells and cell culture. Novikoff rat hepatoma cells (N1S1-67) and mouse L cells were propagated in Swim's medium 67 and enumerated with a Coulter counter as described previously [8,9]. A thymidine kinase-deficient subline of Novikoff cells (1-4-14) was isolated in the same manner as described for subline 1-4-8 [10]. A thymidine kinase-deficient subline of mouse L cells, first isolated by Kit et al. [11], was kindly supplied by Dr. W. Munyon. Mouse leukemia P388, human HeLa and Chinese hamster ovary cells (CHO) were propagated in suspension culture in Eagle's minimal essential medium with spinner salts supplemented with non-essential amino acids and 10% (v/v) fetal calf serum.

Chemicals. Radiochemicals were obtained from the following sources: [*methyl*-^{3}H]thymidine (10 Ci/mmol) from ICN (Irvine, CA); [*carboxy*-^{14}C]-carboxylinulin (2.6 Ci/g) and ^3H_2O (1 mCi/g) from New England Nuclear (Boston, MA). Natural nucleosides, halogenated derivatives, purine riboside, 6-mercaptopurine riboside and 6-methylmercaptopurine riboside were obtained from Sigma Chemical Co. (St. Louis, MO). 2′,3′,5′-Trideoxythymidine and 2′,3′,5′-trideoxyadenosine were synthesized [12] by Dr. Harry Hogenkamp of the University of Minnesota. 6-([4-nitrobenzyl]thio)-9-β-D-ribofuranosylpurine was supplied to us by Drs. Carol Cass and Alan R.P. Paterson of the University of Edmonton. Number 550 silicone fluid was purchased from the Dow-Corning Corp. (Midland, MI). Other chemicals were reagent grade from standard suppliers.

Transport assays. Cells were collected from exponential phase cultures by centrifugation at 400 × *g* for about 2 min, and suspended to a concentration of 1.5—3 · 10^7 cells/ml in glucose-containing basal medium (BM42B; Ref. 13). Alternatively, cells were resuspended in glucose-free basal medium (BM42A) supplemented with 5 mM KCN and 5 mM iodoacetate, and incubated at 37°C for 10 min to deplete them of ATP [10]. Cells suspended in BM42B retained their transport characteristics 3 h or more; cells depleted of ATP were more fragile and were used within 1 h [2].

The rapid kinetic technique for transport measurements has been described in detail elsewhere [2]. In brief, 448 μl of a suspension of cells were rapidly mixed with 61 μl of a solution of radioactive thymidine at short time intervals by means of a hand-operated, dual syringe apparatus. The mixtures emerging

from the mixing chamber were dispensed into 12 tubes mounted in an Eppendorf model 3200/30 microcentrifuge (Brinkmann Instruments, Westbury, NY). The tubes contained 100 μl of an oil mixture consisting of 84 parts silicone fluid No. 550 to 16 parts light mineral oil, by weight (final density = 1.034 g/ml). After the last sample had been mixed, the centrifuge was started, and within an estimated 2 s the cells had entered the oil phase thus terminating transport. When more than 12 sampling times were required, or for sampling times in excess of 2 min, cells and substrate were mixed in the same proportions as provided by the mixing apparatus, and 509-μl samples were removed at appropriate times and centrifuged through oil.

After centrifugation the supernatant medium was aspirated. The upper part of the tube was washed once with water, which was subsequently removed together with most of the oil. 0.2 ml of 0.5 N trichloroacetic acid was added to the tube, and immediately vortexed to disperse the pellet. After 30 min of incubation at 70°C the entire tube and its contents were transferred to a vial containing 8 ml of a modified Bray's solution [8] and analyzed for radioactivity in a liquid scintillation spectrometer. If not specified otherwise, cell suspensions, substrate solutions and apparatus were at ambient temperature, 23–25°C. To study temperature dependence of transport, apparatus and solutions were kept in a thermostated compartment, and thermally equilibrated at the temperature indicated.

Total water space and extracellular space in cell pellets obtained by centrifuging cells through the oil phase were determined in parallel runs in which substrate was replaced by [^{14}C]carboxylinulin in $^{3}H_2O$. All uptake data were corrected for substrate radioactivity in the extracellular space of the cell pellets, and normalized to rates/μl cell water. As indicated in Table I, intra- and extracellular space varied with cell line, but both were proportional to cell number, and the extracellular space was <25% of total water space in the pelleted cells.

TABLE I

EXTRA- AND INTRACELLULAR SPACES OF VARIOUS CELL TYPES AFTER CENTRIFUGATION THROUGH SILICONE OIL

Exponentially growing cells were suspended in basal medium 42B at approximately 10^8 cells/ml, and five dilutions were prepared covering a 20-fold range. The cells were then mixed with [*carboxy*-^{14}C]carboxylinulin and $^{3}H_2O$, equilibrated for about 2 min, and centrifuged through silicone oil, as described in Materials and Methods. Cell-associated radioactivity was determined by dual-channel scintillation counting, and the data were analyzed by linear regression of inulin and water space as a function of the number of cells in the pellet. Volumes/10^6 cells are from the slopes of the regression lines ± the standard error of those slopes. The regression lines passed, within the limits of confidence, through or slightly below the origin. Typical extracellular and intracellular spaces in Chinese hamster ovary cell pellets were 0.28 and 1.3 μl/10^6 cells, respectively, and in HeLa cell pellets, 0.37 and 1.9 μl/10^6 cells, although we have not assayed serial dilutions of these two cell lines.

Cell type	Intracellular space (μl/10^6 cells)	Extracellular space	
		μl/10^6 cells	% of total
N1S1-67, Novikoff rat hepatoma	1.36 ± 0.01	0.24 ± 0.1	14.8
L cells, mouse fibroblast	2.31 ± 0.07	0.41 ± 0.1	15.2
P388, mouse leukemia	0.95 ± 0.03	0.30 ± 0.02	24.2

Integrated, zero-trans rate equations. Eilam and Stein [5] have derived a general rate equation for a simple, carrier-mediated, non-concentrative transporter. We have previously noted [2] that for influx of substrate from an infinitely large pool into a cell this rate equation may be integrated over time and rearranged in the form of an implicit function with respect to intracellular concentration:

$$S_{2,t} = S_1\left[1 - \exp\left(\frac{-t - f_2(S_1, S_{2,t})}{f_1(S_1)}\right)\right] \tag{1}$$

where $S_{2,t}$, concentration of substrate on side 2 of the cell membrane (for our purposes, the inside) at time t ($S_{2,0} = 0$); S_1, substrate concentration on side 1 (outside) and is taken as constant; and f_1 and f_2 are functions of various kinetic parameters, and are defined in Eqns. 3 and 4. If f_2 is neglected (in fact, $f_2 \to 0$, as $t \to 0$, and becomes constant as $t \to \infty$), Eqn. 1 becomes equivalent to the integrated equation of a first-order reaction:

$$S_{2,t} = S_1[1 - \exp(-k't)] \tag{2}$$

where $k' = 1/f_1$. When $S_1 << K_{12}^{zt}$, f_2 is indeed insignificant, so that Eqn. 2 describes the influx of substrate under this condition; this, of course, is the condition in which influx is first order with respect to substrate concentration.

In view of the rapidity of nucleoside influx into mammalian cells, it is advantageous (and in our experience practically essential) to compute initial velocity of transport from the time course of appearance of substrate intracellularly by means of such integrated equations. For the sake of mathematical simplicity, we have previously employed Eqn. 2 to estimate initial velocities of transport [1,14], though it has become clear that neglect of the f_2 term leads to a progressive underestimation of initial velocity as exogenous substrate concentration increases above the Michaelis-Menten constant for transport (see Results). In this paper we have used exact equations in the form of Eqn. 1 to estimate initial velocities from the time course of approach to transmembrane equilibrium. Solution of such equations requires iterative techniques and are practicable only with a computer's aid. We have set $S_{2,t}$ on the right-hand side of Eqn. 1 initially to zero, solved for $S_{2,t}$, and reset $S_{2,t}$ (right-hand side) at this new value and solved again. Iteration was continued until $S_{2,t}$ on the left- and right-hand sides were equal to within 12 digits. The value for $S_{2,t}$ thus obtained uniquely satisfies the equation.

Degree of symmetry in transport models. In the nomenclature of Eilam and Stein [5] functions f_1 and f_2 in Eqn. 1 are:

$$f_1(S_1) = KR_{00} + R_{12}S_1 + R_{21}S_1 + S_1^2R_{ee}/K \tag{3}$$

and

$$f_2(S_1, S_{2,t}) = (R_{21} + R_{ee}S_1/K)S_{2,t} \tag{4}$$

where K is substrate : carrier dissociation constant and is related to the Michaelis-Menten constants apparent in various experimental protocols by ratios of appropriate R terms; the R terms are resistance factors, proportional to the times of a round-trip for the carrier in one of four modes: (i) loaded on the inbound trip and empty on the outbound (R_{12}); (ii) empty on inbound and

loaded on outbound (R_{21}); (iii) empty in both directions (R_{00}), or (iv) loaded in both directions (R_{ee}). Necessarily $R_{00} + R_{ee} = R_{12} + R_{21}$. The reciprocals of R terms are equal to the corresponding maximal velocities; for example, the maximal velocity of zero-*trans* influx = $V_{12}^{zt} = 1/R_{12}$, and the maximal velocity of equilibrium exchange of isotopic substrate = $V^{ee} = 1/R_{ee}$.

Functional symmetry of the carrier is manifest as equivalence of various R terms. If carrier movement is indifferent with respect to direction ('in/out symmetry'), $R_{12} = R_{21}$. If the loaded carrier moves as rapidly as the unloaded, $R_{ee} = R_{00}$. One can impose such symmetry constraints on the solution to Eqn. 1 with the effect of reducing the number of kinetic parameters to be fit to a given set of data. Once the values for K and the R parameters are obtained by least-squares fitting procedures, initial velocities may be calculated according to Eilam and Stein's differential rate equation with $S_2 = 0$ (written here in the form of the Michaelis-Menten equation):

$$v_{12}^{zt} = \frac{S_1/R_{12}}{KR_{00}/R_{12} + S_1} \tag{5}$$

Equilibrium exchange and infinite-trans protocols. To measure the rates of isotope exchange in the absence of net flux ('equilibrium exchange'), thymidine kinase-less cells were preincubated with the desired concentration of unlabeled thymidine. Samples of this suspension were then mixed, as described above, with thymidine at the same concentration, but tritiated. The appearance of radioactivity in the sedimented cells corresponds to a change of specific radioactivity in intracellular thymidine, and is described as a function of time by Eilam and Stein [5]:

$$N_{2,t} = N_{2,\infty}\left[1 - \exp\left(-\frac{V^{ee}t}{K^{ee} + S}\right)\right] \tag{6}$$

where $N_{2,t}$, intracellular radioactivity at time t, and is proportional to the specific radioactivity of intracellular substrate; $N_{2,\infty} = N_1$ = radioactivity/equivalent volume of medium; S, concentration of substrate, and K^{ee} and V^{ee} are the apparent Michaelis-Menten constants for equilibrium exchange. Eqn. 6 is made formally identical to Eqn. 2 by substituting $V^{ee}/(K^{ee} + S) = k'$. K^{ee} and V^{ee} were evaluated by replots of k' versus S, fit by the least-squares procedure.

An 'infinite-*trans*' experiment involves countertransport of exogenous radiolabeled substrate at a given concentration against non-labeled substrate present intracellularly at very high concentration. Dual syringe methodology is not well suited to an infinite-*trans* protocol. Instead, cells were preloaded with 10 mM thymidine for 30 min. The equilibrated cells were then collected by centrifugation and washed rapidly in basal medium at 0°C by resuspension and centrifugation. The cells were then resuspended to their original density in medium containing varying concentrations of labeled substrate. At various times of incubation, duplicate 0.5 ml samples were layered over oil and centrifuged in an Eppendorf centrifuge. The initial rate of entry of labeled substrate was estimated graphically from the initial linear portion of the uptake curve. Apparent Michaelis-Menten parameters were estimated for plots of initial entry rates versus concentration of labeled substrate.

Statistical treatment of data. Eqn. 1, with appropriate symmetry constraints,

has been fit by the methods of least-squares to pooled data comprising measured intracellular substrate concentrations ($S_{2,t}$) at 12 or more times (t) for each of several exogenous substrate concentrations (S_1). Since we use equal radioisotope concentration irrespective of total substrate concentration, we consider data collected at low substrate concentrations to be as reliable as those at high concentrations. For purposes of least-squares fitting, this judgement is accommodated by weighting the data as the reciprocal of substrate concentration.

The standard error of estimate for any given kinetic constant was computed from the variances and covariances of the best-fitting K and R parameters in Eqn. 1 as outlined by Cleland [15]. Kinetic constants are expressed ± S.E.

The significance of the improvement in fit achieved by removing symmetry constraints was evaluated by an F-test as described by Pollard [16].

In some instances initial zero-*trans* velocities had to be estimated from influx data at a single concentration of substrate. As a rule, the iterative least-squares computation converged in these instances only if all R values of Eqns. 3 and 4 were set equal (the justification for this constraint is discussed below), and if either the R parameter or K was fixed at a known value. For example, the velocities reported in Table VI were obtained by fixing the value of R in the presence of inhibitor to that found in the absence of inhibitor. The initial zero-*trans* velocities of Fig. 5 were computed with K fixed at values interpolated from Table IV. In fact, the initial velocities so calculated are relatively insensitive to the value at which a parameter is fixed. In the latter example, doubling the value at which K was fixed decreased the calculated initial velocities by <25%.

All computations reported here were carried out on a Hewlett-Packard (Loveland, CO) 9825A desktop computer equipped with a 9871A printer. Curve-fitting programs were developed on the algorithm of Dietrich and Rothmann [17]; the authors will honor requests for program listings.

Results

The time course of thymidine influx

Fig. 1 illustrates the adequacy with which Eqn. 1 described the time course of thymidine entry into thymidine kinase-deficient Novikoff hepatoma cells. Note that at substrate concentrations much less than the calculated Michaelis-Menten constant (panels A and B), half-equilibrium, and consequently a 50% decrease from true initial velocity, occurred with 10 s even at 24°C.

The zero-*trans* rate equation fit to these data was that in which all the R values of Eqns. 3 and 4 were held equal (full symmetry). In fact, all the zero-*trans* kinetic data comprising this study were fit also with R_{12} kept equal to R_{21} (in/out symmetry), and with no symmetry constraints at all. In no case was the improvement in fit realized by removing symmetry constraints significant, as judged by the F-statistic; generally the probability of the null hypothesis exceeded 0.8.

Close examination of Fig. 1 discloses that, as exogenous concentration increased, the shape of the zero-*trans* curve diverged from that of a simple, first-order approach to equilibrium. This divergence, and the inadequacy of a

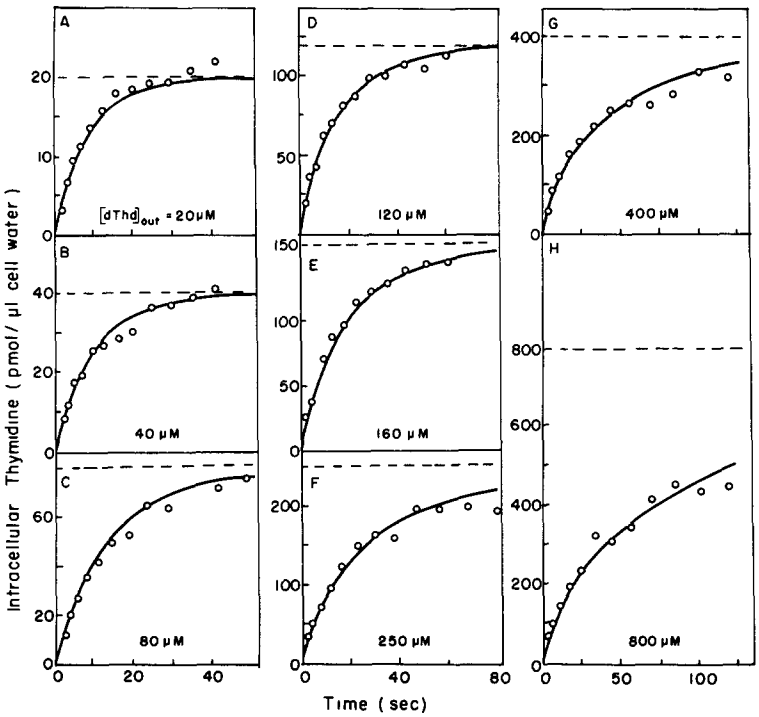

Fig. 1. Zero-*trans* influx of thymidine in thymidine kinase-deficient Novikoff hepatoma cells as fit by an integrated rate equation. Cells were harvested at $1.2 \cdot 10^6$/ml and resuspended in basal medium 42B at $2.2 \cdot 10^7$ cells/ml. The appearance of radioactivity from exogenous [^{3}H]thymidine (773 cpm/μl of final suspension, irrespective of concentration) within cells was followed at short time intervals by means of the dual syringe/oil centrifugation technique described in Materials and Methods. Radioactivity/cell pellet was converted to pmol/μl intracellular water on the basis of measured [^{14}C]inulin space (=1.76 μl/cell pellet, assumed to equal extracellular water space) and total ^3H_2O space (=15.3 μl/cell pellet). The symmetrical, zero-*trans* integrated rate equation (Eqn. 1, with all R parameters held equal) was fit to these data whereby time (t) and exogenous thymidine concentration (S_1) were treated as independent variables, and intracellular concentration ($S_{2,t}$) as dependent variable. The best-fitting parameters were $K = 168 \pm 7.8$ μM ($=K_{12}^{zt}$) and $R = 0.0458 \pm 0.0007$ (μl · s)/pmol ($=1/V_{12}^{zt}$). The correlation coefficient, $r_{y,\hat{y}} = 0.9915$. The curves drawn are the theoretical ones for zero-*trans* influx at these parameter values with S_1 at concentrations indicated. ------, expected equilibrium level based on the measured intracellular water space.

simple, exponential equation in estimating initial entry velocities at substrate concentrations high relative to K_{12}^{zt} may be better appreciated in Fig. 2. There, both Eqn. 1 (integrated zero-*trans* with full symmetry) and Eqn. 2 (integrated first order with S_1 replaced by $S_{2,\infty}$ and treated as a parameter to be fit) are fit to the same data, viz. for zero-*trans* influx with exogenous thymidine = 4000 μM. Although superficially Eqn. 2 seems to fit the data fairly well, two artifacts become apparent on closer inspection. (i) the asymptote arrived at would imply an intracellular substrate space considerably less than the measured intracellular water space (dashed line). (ii) The early time points (see inset of Fig. 2) are poorly accommodated, with the consequence that the slope of the influx curve at zero time is less than half that for the zero-*trans* curve. We have previously employed the exponential equation to estimate initial

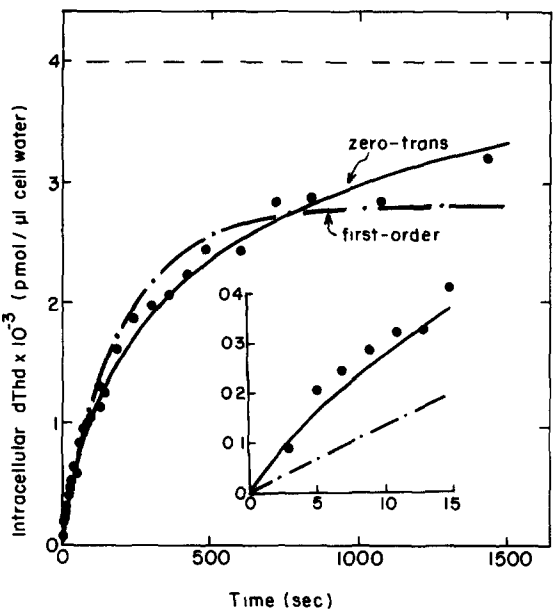

Fig. 2. Adequacy of zero-*trans* and first-order equations to describe influx at high thymidine concentrations. Novikoff hepatoma cells (thymidine kinase deficient) were harvested at $1.3 \cdot 10^6$ cells/ml, resuspended at $3.5 \cdot 10^7$ cells/ml in basal medium and monitored for [^{3}H]thymidine influx (4000 µM, 0.48 cpm/pmol) as described in Materials and Methods, except that three runs at twelve samples each were made to cover the time range from 1 s to 24 min. Raw data were converted to pmol/µl cell water (extracellular space, 3.3 µl/pellet; intracellular space, 29.5 µl/pellet) and fit by the symmetrical, zero-*trans* integrated rate equation (Eqn. 1 in text, all R parameters held equal) (———) and by the first-order integrated rate equation (Eqn. 2 in text, whereby S_1 was replaced by $S_{2,\infty}$ and treated as a parameter to be fit) (· — · — ·). The calculated initial velocities were 43.3 pmol/s per µl water (residual mean square = 6740) for the zero-*trans* fit and 13.5 pmol/s per µl cell water (residual mean square = 28 700) for the first-order fit. The inset shows the same two curves enlarged over the first 15 s. - - - - - -, expected equilibrium level based on intracellular water space.

velocities of zero-*trans* influx even at high concentrations of substrate. As a consequence K_{12}^{zt} and V_{12}^{zt} reported earlier [1,18] are consistently less than those given in Table II.

Increasing awareness of these artifacts motivated our efforts to apply theoretically more rigorous equations to the analysis of zero-*trans* influx data than we had been able to do heretofore.

Zero-trans kinetics in various cell lines

The data presented in Fig. 1 have been reduced to two parameters, viz. the best-fitting values for K_{12}^{zt} and V_{12}^{zt}. These values contribute one line to Table II, which summarizes the zero-*trans* kinetic parameters (23—25° C) found using five different cell lines and two different methods of eliminating thymidine metabolism.

Noteworthy is (i) that the kinetic values obtained with the kinase-less cells were comparable to those in their wild-type counterparts, and (ii) that kinase-less mutants of Novikoff cells manifest similar transport properties whether they were subjected to KCN/iodoacetate treatment or not. Variation in culture pH may contribute to variability in measured transport rate (Fig. 3). Variation

TABLE II

KINETIC PROPERTIES OF THYMIDINE TRANSPORT IN VARIOUS CELL SYSTEMS

Zero-*trans* influx of [^{3}H]thymidine was measured at 23—25°C over a concentration range of 5—800 μM in various cell lines by the dual syringe technique described in Materials and Methods. To suppress metabolism cells were treated, where indicated, with 5 mM KCN and 5 mM iodoacetate, which depletes cellular ATP. The kinetic parameters were obtained by fitting the symmetrical, zero-*trans* integrated rate equation to the pooled data for isotope influx, as exemplified in Fig. 1, and are expressed ± S.E. of estimate. Each line of the table represents a separate experiment with a different batch of cells and encompasses data at twelve or more time points for each of six or more concentrations of thymidine.

Cell line	Depleted of ATP	K_{12}^{zt} (μM)	V_{12}^{zt} (pmol/s per μl cell H_2O)
N1S1-67 (wild type)	yes	245 ± 28	60 ± 3
N1S1-67 (TK$^-$) *	no	262 ± 10	41 ± 1
	no	266 ± 19	27 ± 0.7
	no	278 ± 12	21 ± 0.4
	no	207 ± 15	27 ± 0.7
	no	168 ± 8	22 ± 0.3
	no	163 ± 8	17 ± 0.3
	yes	233 ± 7	32 ± 0.4
	average:	228	27
L cells (wild type)	yes	141 ± 7	10 ± 0.2
L cells (TK$^-$) *	no	177 ± 17	32 ± 1
	no	103 ± 5	16 ± 0.3
CHO (wild type)	yes	96.6 ± 3.4	5.0 ± 0.09
	yes	86.7 ± 5.2	5.2 ± 0.12
	yes	104 ± 3	9.3 ± 0.11
	yes	112 ± 5	7.2 ± 0.13
	yes	117 ± 3	7.4 ± 0.07
	average:	103	6.8
P388	yes	125 ± 10	21 ± 0.7
HeLa	yes	125 ± 5	8.2 ± 0.1

* TK$^-$, thymidine kinase deficient.

of transport velocity with growth phase of a culture is not a contributing factor [19].

Exchange of isotopic thymidine across Novikoff cell membranes

From the values of the kinetic constants obtained in zero-*trans* experiments, and from the conclusion that zero-*trans* data are adequately described when the resistivities (R parameters) to transporter movement are held equal regardless of whether the transporter is loaded or unloaded, inbound or outbound, one can predict that the apparent Michaelis-Menten parameters of isotope exchange should equal those for zero-*trans* influx. This argument holds both for exchange when thymidine concentrations inside and outside are varied together (equilibrium exchange) or when unlabeled thymidine inside is held at a constant, high concentration, while exogenous, labeled thymidine is varied (infinite-*trans*).

Experimental confirmation of these predictions is summarized in Table III. The results of four equilibrium exchange experiments at ambient temperature (23—25°C) are itemized in the table. An example of these experiments may be seen in Fig. 6A and C (discussed below in context of temperature dependence), from which is taken line three of Table III. The tabulated values for K_{12}^{it} and V_{12}^{it} are taken from the experiment shown in Fig. 4.

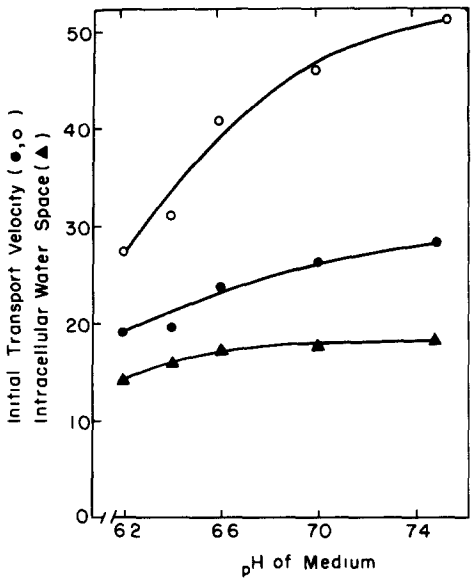

Fig. 3. Effect of extracellular pH on initial velocity of thymidine influx. Thymidine kinase-deficient Novikoff hepatoma cells were resuspended at $2.7 \cdot 10^7$ cells/ml in five flasks containing glucose-free basal medium initially adjusted to span pH 6—8. Each suspension was preincubated for 10 min, then the initial velocity of thymidine transport was determined with an aliquot of the suspension using the double syringe technique, final thymidine concentration was 325 μM, 835 cpm/μl. The pH was determined just before and after incubation with thymidine in separate flasks to which cell suspension and thymidine solution were added in the same proportions as achieved by the double syringe apparatus. During this time it changed not more than 0.15 pH unit; the final pH is reported. Extracellular (not shown) and intracellular (▲, μl/cell pellet) water spaces were determined in triplicate, at each pH, for aliquots the cell suspension centrifuged through oil (see Materials and Methods). Initial velocities were obtained by fitting the symmetrical zero-*trans* integrated rate equation to the data with K held at 225 μM, and using the best-fitting value for R to calculate initial velocity at S_1 = 325 μM, according to Eqn. 5. Initial velocities were normalized to intracellular volume (○, pmol/s per μl cell water) and cell number (●, pmol/s per 10^6 cells).

TABLE III

KINETICS OF THYMIDINE ISOTOPE EXCHANGE IN NOVIKOFF HEPATOMA CELLS

Flux of thymidine radioisotope was measured at 23—25°C with the equilibrium exchange and infinite-*trans* protocols described in Materials and Methods. The kinetic parameters of equilibrium exchange were determined in four separate experiments like that portrayed in Fig. 6A and C. Those for infinite-*trans* were computed for the experiment shown in Fig. 4. For comparison zero-*trans* kinetic parameters are also given. These are the means (± S.D.) of those experiments of Table II done with N1S1-67 Novikoff rat hepatoma cells.

Experimental design	K_m (μM)	V (pmol/s per μl cell H_2O)
Equilibrium exchange	368 ± 55	73 ± 8
	312 ± 82	42 ± 9
	181 ± 23	29 ± 3
	231 ± 131	40 ± 18
averages:	273	46
Infinite-*trans*	246 ± 41	71 ± 4
Zero-*trans*	228 ± 16	31 ± 5

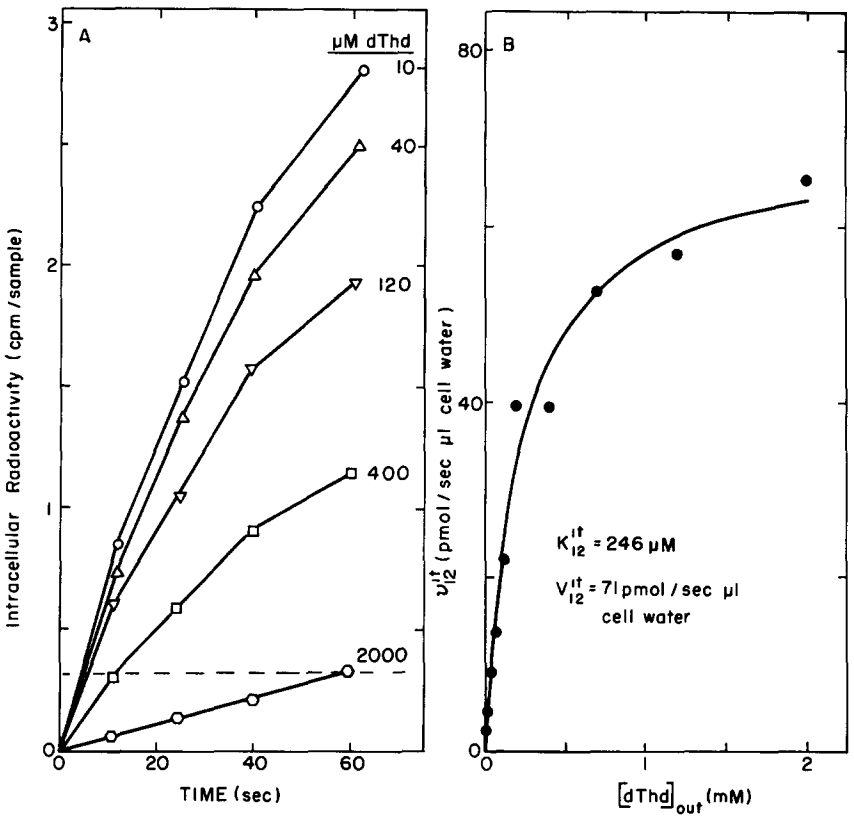

Fig. 4. Infinite-*trans* transport of thymidine in thymidine kinase-deficient Novikoff hepatoma cells. Cells were preloaded with 10 mM thymidine for 30 min. Aliquots of the equilibrated cells were then collected by centrifugation. The cells were resuspended in medium containing [^{3}H]thymidine (246 cpm/μl, irrespective of concentration) at one of ten concentrations ranging from 10 to 2000 μM. After 12, 25, 40 and 60 s of incubation at 24°C duplicate 0.5 ml samples of the suspension were layered over oil and centrifuged. Panel A shows the time courses of appearance of radioactivity in the cell pellets (for purposes of clarity only five concentrations are shown). Initial velocities were estimated from the 12 s point, and are plotted against concentration of exogenous thymidine in panel B. The curve is that corresponding to best-fitting Michaelis-Menten parameters.

Temperature dependence of thymidine influx and exchange

Arrhenius plots of thymidine uptake into wild-type Novikoff hepatoma cells shows a discontinuity at 17—23°C [20]. The recent results, noted in the Introduction, which demonstrate phosphorylation to be the rate-determining step of thymidine uptake (at least at temperatures ⩾23°C), suggested, however, that the break in the Arrhenius plot of uptake velocity might not be attributable to discontinuous behavior of the thymidine transporter with respect to temperature. Accordingly, we have examined the temperature dependence of thymidine transport in thymidine kinase-deficient Novikoff hepatoma cells under three experimental conditions (Fig. 5): (i) with zero-*trans* protocol at 5 μM exogenous thymidine; (ii) with zero-*trans* protocol near (approx. 78% at 24°C) saturation of the carrier, and (iii) with equilibrium exchange protocol near (83%) saturation. The similarity of entry and exchange velocities observed

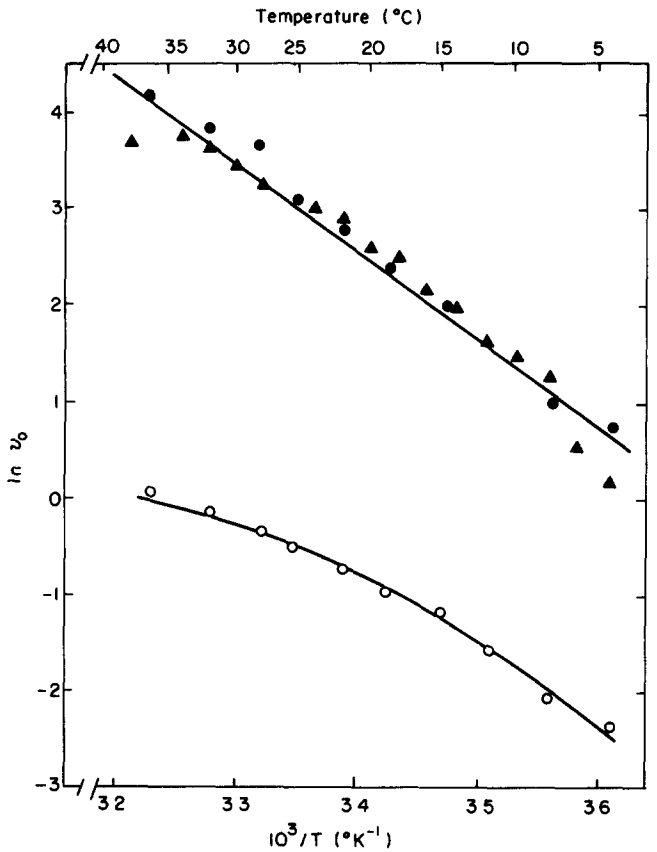

Fig. 5. Temperature dependence of thymidine influx and exchange. Suspensions of thymidine kinase-deficient Novikoff cells (at about $3 \cdot 10^7$ cells/ml basal medium) were assayed for zero-*trans* influx of [^{3}H]thymidine at 5 μM (○) or 800 μM (●) and for isotopic exchange with cells preincubated at 1330 μM (▲) as described in Materials and Methods. Cell suspensions, substrate solutions and apparatus were thermally equilibrated before assay at the temperature indicated on the upper abscissa. The time course of appearance of radioisotope in the cell pellets was followed with 12 samplings encompassing 39—234 s, depending on temperature and concentration. Initial velocities were computed by fitting a first-order integrated rate equation to equilibrium exchange data (Eqn. 6 in text) and to influx data at 5 μM thymidine (Eqn. 2 in text), or by fitting the symmetrical zero-*trans* integrated rate equation (Eqn. 1 in text with all R parameters equal) to influx data at 800 μM thymidine, whereby $K_{\frac{1}{2}}^t$ was held at values interpolated from Fig. 7. The computed initial velocities are plotted against inverse absolute temperature. The upper curve is the regression line on pooled influx and exchange data and corresponds to an Arrhenius activation energy of 18.3 kcal/mol.

at 23°C (see Table III) was seen here to extend over the full range of temperature accessible with viable cells. Thus zero-*trans* and equilibrium exchange data were essentially coincidental, and have been pooled to determine an Arrhenius activation energy of 18.3 kcal/mol (corresponding to $Q_{10} = 2.7$ for 25—35°C). There was no evidence for a biphasic curve at near-saturating substrate concentrations.

The perceptible curvature at sub-K_{12}^{zt} concentration of thymidine is probably due to an increase in K_{12}^{zt}, with a resultant decrease in fractional saturation at 5 μM, with temperature (see Table IV).

The apparent Michaelis-Menten constants for zero-*trans* influx and equilibrium exchange are functions of the carrier : substrate dissociation constant (K) and the ratios of appropriate resistivities [5], viz.

$$K_{12}^{zt} = KR_{00}/R_{12} \tag{7}$$

and

$$K^{ee} = KR_{00}/R_{ee} \tag{8}$$

Since experiments described in the previous section had indicated that, at 23—25°C, $R_{00} = R_{12} = R_{ee}$, we anticipated that the equivalence might hold over a range of temperature. If so, K_{12}^{zt} and K^{ee} should exhibit similar temperature dependence, and the slope of the van't Hoff plot ($\ln K$ vs. $1/T$) should be proportional to the enthalpy of carrier : substrate dissociation.

The results of equilibrium exchange experiments at 6, 25 and 37°C in thymidine kinase-less Novikoff hepatoma cells are presented in Fig. 6. Zero-*trans* experiments were conducted also at 4, 24 and 37°C (the time courses are not shown), and the kinetic parameters obtained from least-squares fits of the

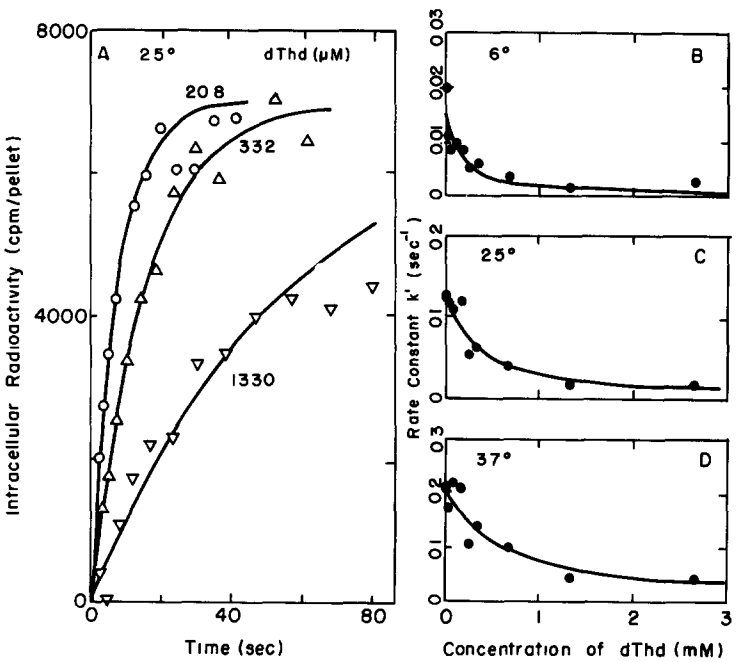

Fig. 6. Kinetics of thymidine (dThd) equilibrium exchange as a function of temperature. Novikoff hepatoma cells deficient in thymidine kinase were suspended at $2.5 \cdot 10^7$ cells/ml in basal medium, divided into ten flasks, and preincubated for 10 min at 37°C with non-radioactive thymidine at various concentrations ranging from 5 to 2660 μM. The time course of isotope exchange was followed with aliquots from each flask mixed with [^{3}H]thymidine (780 cpm/μl, irrespective of concentration) at the same concentration used for preincubation (see Materials and Methods), but with solutions and apparatus equilibrated in turn at 6, 25 and 37°C. Panel A gives examples of time courses at 25°C and 20.8 (○), 332 (△), and 1330 (▽) μM thymidine, and the best-fitting curves of the form of Eqn. 2 (see text). Panels B—D replot the first-order rate constants thus obtained against concentration of thymidine for 6, 24 and 37°C, respectively, according to the relationship $k' = V^{ee}/(K^{ee} + S)$ as elaborated in the text. Values for V^{ee} and K^{ee} (± S.E. of estimate) are tabulated in Table IV.

TABLE IV

TEMPERATURE DEPENDENCE OF K AND V FOR ZERO-*trans* INFLUX AND EQUILIBRIUM EXCHANGE

Influx of [^{3}H]thymidine at ten concentrations between 2.5 μM and 2.5 mM was measured in thymidine kinase-deficient Novikoff hepatoma cells as described in Materials and Methods, but at ambient temperatures of 4, 24 and 37°C. K_{12}^{zt} and V_{12}^{zt} were computed from the pooled time course data by means of the symmetrical zero-*trans* integrated rate equation as exemplified in Fig. 1. K^{ee} and V^{ee} are tabulated for the equilibrium exchange experiment shown in Fig. 6.

Experimental design	Temp. (°C)	Kinetic constants	
		K (μM)	V (pmol/s per μl cell H_2O)
Zero-*trans*	4	66.7 ± 44	1.25 ± 0.03
	24	207 ± 15	27.4 ± 0.7
	37	420 ± 8	92.4 ± 0.8
Equilibrium exchange	6	134 ± 58	22 ± 0.8
	25	312 ± 82	42 ± 9
	37	572 ± 197	123 ± 36

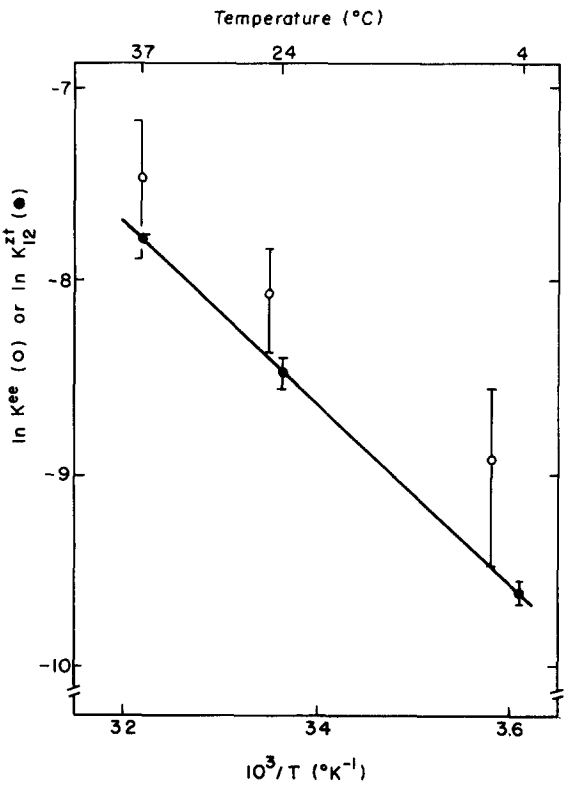

Fig. 7. Temperature dependence of $K_{\frac{1}{2}}^{zt}$ and K^{ee}. Values for K^{ee} (expressed in molarity and with range lines indicating standard error of estimate) are taken from the experiment shown in Fig. 6. Values for $K_{\frac{1}{2}}^{zt}$ are taken from Table IV. These values are plotted to illustrate the van't Hoff relationship: $d(\ln K_{eq})/d(1/T) = -\Delta H^{0\prime}/R$ (where R is the universal gas constant, T is the absolute temperature, and $-\Delta H^{0\prime}$ is the enthalpy of the reaction characterized by K_{eq}.) The line shown is the regression line on $\ln K_{12}^{zt}$, and corresponds to an enthalpy of carrier : substrate dissociation equal to 9.3 kcal/mol. Since the apparent free energy of dissociation at 24°C is 5 kcal/mol (=$-RT \ln K$, see Table III), this yields an entropy of dissociation of 15 cal/deg. per mol.

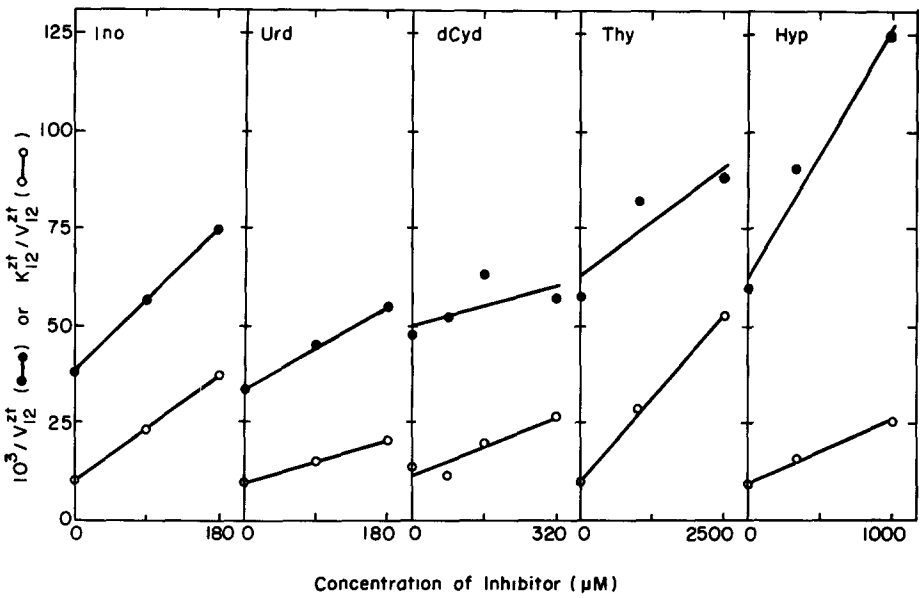

Fig. 8. Kinetic analysis of inhibition of thymidine influx by other nucleosides and nucleic acid bases. The influx of [^{3}H]thymidine into thymidine kinase-deficient Novikoff hepatoma cells was measured in sixteen experiments similar to the one portrayed in Fig. 1. In addition to [^{3}H]thymidine, however, a non-labeled inhibitor was present in the substrate solution to give the final concentrations indicated on the abscissas. For each experiment an apparent K_{12}^{zt} and V_{12}^{zt} was computed by fitting the symmetrical, zero-*trans* integrated rate equation to the pooled data of that experiment (as exemplified in Fig. 1). For each inhibitor, $1/V_{12}^{zt}$ (●) and K_{12}^{zt}/V_{12}^{zt} (○) are plotted against [I], so that the x-intercept gives, respectively, $K_{i,intercept}$ and $K_{i,slope}$ (see Ref. 21). The x-intercepts were calculated by regression analysis and are tabulated with the associated standard errors of estimate in Table V.

respective rate equations to data from both experiments are tabulated in Table IV. As with zero-*trans* data collected at 23—25° C, here too the symmetrical zero-*trans* equation fit the data well; no significant improvement in fit was realized by removing the symmetry constraint. Although the kinetic parameters of equilibrium exchange seem consistently higher than those of zero-*trans*, the errors of estimate of the former were large, and it is apparent from Fig. 7 that the temperature dependence of the two parameters were similar. The linearity of these van't Hoff plots (Fig. 7) indicates that the apparent enthalpy (9.3 kcal/mol) of carrier : substrate dissociation was constant over the temperature range 4—37° C.

Specificity of the thymidine transporter

We have examined in Novikoff hepatoma cells the inhibtion of thymidine influx by several nucleosides and nucleic acid bases in an effort to delineate the specificity of the thymidine transport sytem. For five substances, inosine, uridine, deoxycytidine, thymine and hypoxanthine, the pattern of inhibition has been extensively characterized, i.e. the initial velocities of thymidine transport have been determined as a function of exogenous thymidine concentration at two or three concentrations of inhibitor. In each case the symmetrical, integrated zero-*trans* rate equation was fit to the data to yield best-fitting values of K_{12}^{zt} and V_{12}^{zt}. Subsequently $1/V_{12}^{zt}$ and K_{12}^{zt}/V_{12}^{zt} were plotted against con-

TABLE V

SUMMARY OF INHIBITION CONSTANTS FOR THYMIDINE INFLUX

Values given are the x-intercepts (± S.E. of estimate), obtained by linear regression, for the replots of $1/V_{12}^{zt}$ versus [I] (x-cept = $K_{i,intercept}$) and K_{12}^{zt}/V_{12}^{zt} versus [I] (x-cept = $K_{i,slope}$) shown in Fig. 8.

Inhibitor	Inhibition constants (μM)	
	$K_{i,intercept}$	$K_{i,slope}$
Inosine	192 ± 44	64 ± 4
Uridine	394 ± 7	156 ± 24
Deoxycytidine	1620 ± 1560	232 ± 113
Thymine	5610 ± 3130	593 ± 92
Hypoxanthine	1000 ± 252	609 ± 152

TABLE VI

INHIBITORS OF THYMIDINE INFLUX IN NOVIKOFF HEPATOMA CELLS

Inhibition of thymidine influx by a number of compounds was screened in three separate experiments with Novikoff hepatoma cells. In Exp. 1 concentration of substrate ([^{3}H]thymidine) was 320 μM and the initial velocity of entry v_{12}^{zt},control was 23.2 pmol/s per μl cell water; in Exp. 2, substrate = 160 μM and v_{12}^{zt},control = 8.14 pmol/s per μl cell water; in Exp. 3, substrate = 120 μM and v_{12}^{zt},control = 14.6 pmol/s per μl cell water. Since the condition $S_1 << K_{12}^{zt}$ was not met in any of these experiments, initial velocities were determined by fitting the symmetrical, zero-*trans* integrated rate equation to the data for a single concentration of substrate, whereby R_{12} (= $1/V_{12}^{zt}$) was held at a value taken as a average of duplicate controls. This procedure is tantamount to assuming competitive inhibition, but was necessary to fit the data successfully with the zero-*trans* equation. The values obtained for initial velocities (v_{12}^{zt},inhibitor) are little affected by this assumption; however, the best-fitting value for apparent K_{12}^{zt} in the presence of inhibitor, or for a K_i derived from it, would be invalid (and is therfore not reported) to the extent that inhibition is probably not strictly competitive (see Fig. 8).

Inhibitor	Conc. of inhibitor (μM)	v_{12}^{zt},inhibitor/v_{12}^{zt},control
Expt. 1		
5′-Bromodeoxyuridine	320	0.27
	3200	0.07
Deoxyinosine	320	0.38
Deoxyuridine	320	0.39
	3200	0.07
Expt. 2		
Cytosine	160	1.3
	800	0.98
Uracil	160	0.94
	800	0.56
D-Ribose	160	1.0
	800	0.75
Expt. 3		
Purine riboside	120	0.18
	480	0.06
6-Mercaptopurine riboside	120	0.58
	480	0.28
6-Methylmercaptopurine riboside	120	0.14
	480	0.04
2′,3′,5′-Trideoxyadenosine	120	0.66
	480	0.31
6-([4-Nitrobenzyl]thio)-9-β-D-ribofuranosylpurine	1	0.67
	10	0.10

centration of inhibitor, corresponding to the 'intercept' and 'slope' replots, respectively, conventionally used to characterize inhibitors of enzymatic reactions [21]. These plots are shown in Fig. 8, and the $K_{i,slope}$ and $K_{i,intercept}$ derived from them are listed in Table V. With all five substances both $1/V_{12}^{zt}$ and K_{12}^{zt}/V_{12}^{zt} appear to be related linearly to inhibitor concentration; thus each substance might be classified as a linear, non-competitive inhibitor of thymidine influx. All inhibitors showed a stronger influence on K_m than on V (i.e. $K_{i,slope} < K_{i,intercept}$), while the bases were less effective than the nucleosides.

Twelve additional compounds, including several nucleoside analogs, were tested simply for their ability to inhibit thymidine influx at a single concentration of thymidine (see Table VI). At a concentration of inhibitor equal to that of substrate all of the nucleosides, with the exception of 2',3',5'-trideoxythymidine, inhibited thymidine influx <33%. Cytosine was non-inhibitory, while D-ribose and uracil were weakly inhibitory.

Discussion

The results of this paper, together with a preliminary report on the subject [1], represent the first comprehensive, kinetic characterization of nucleoside transport into cultured mammalian cells, based on methodology adequate to cope with the manifest rapidity of that transport, in cell systems not complicated by metabolism of transported substrate, and interpreted in terms of theoretically derived, integrated rate equations.

Wherever a zero-*trans* experimental protocol was used, three versions of an integrated rate equation were fit to the data, corresponding to three ramifications of a simple, carrier-mediated, non-concentrative model: (i) where the rate of carrier movement was assumed to be different in all modes of movement; (ii) where the rate was assumed different for loaded and empty carrier, but equal with respect to direction of movement, and (iii) where all rates, loaded or empty, in or out, were assumed equal. In every instance the fully symmetrical version (iii) fit the data well; for the results in Table I, for example, the worst correlation between actual intracellular concentrations and those calculated for the best-fitting parameters was 0.96, most were $\geqslant 0.99$. Moreover, in no case did the introduction of the additional parameters necessitated by versions (i) and (ii), significantly improve the fit, as estimated by the F-statistic.

Table II legitimizes, a posteriori, a chemical device we have used to suppress metabolism in cell lines for which thymidine kinase-less mutants were not available to us, namely the depletion of cellular ATP by treatment with 5 mM KCN plus 5 mM iodoacetate. Thus in Novikoff hepatoma cells and in mouse L cells the kinetic characteristics of thymidine transport are comparable with or without ATP depletion, lending confidence to our assumption that ATP depletion is a generally useful procedure for measuring nucleoside transport unencumbered by intracellular phosphorylation. The comparison, of course, also establishes the independence of the thymidine transporter from cellular energy supply.

The K_{12}^{zt} of thymidine transport in these five cell lines is some 200-times the K_m of thymidine uptake described by numerous investigators in several mammalian cell lines ($K_m^{uptake} \approx 0.5\ \mu M$; reviewed in Refs. 22 and 23). This

difference is not a discrepancy in the real sense, but a consequence of uptake's being a multi-step process for which transport is not the rate-determining step [4,19]. In fact, the K_{12}^{zt} values reported here are reminiscent of those reported for thymidine in human red blood cells [24], which are inherently unable to metabolize thymidine.

A further distinction between the present results and conclusions drawn from uptake studies is our failure to detect any significant contribution from 'simple diffusion' (non-mediated permeation) of thymidine. The non-mediated permeation seen in uptake studies is likely an artifact, explicable, in light of the data reported here, as follows. Accumulation of substrate-derived radioactivity in phosphorylating cells comprises two classes of compounds, (i) phosphorylated compounds, the accumulation of which progresses measurably within the time scale employed in most uptake studies, and which shows Michaelian dependence on exogenous substrate concentration, presumably reflecting saturability of thymidine kinase, and (ii) free, intracellular thymidine, which, at the same time scale, appears to be constant and directly proportional to the concentration of exogenous thymidine. If one equates, erroneously, total accumulation per given time as a measure of uptake velocity, and analyzes this 'velocity' as a function of exogenous substrate concentration, one perceives one component apparently saturable and another apparently not.

Conformity of zero-*trans* influx data to the theoretical equation for carrier-mediated influx provides evidence for the correctness of the simple, functionally symmetrical, carrier-mediated transport model, and allows calculation of kinetic parameters defined by this model. The results of the infinite-*trans* and equilibrium exchange experiments (Fig. 4 and Table III) confirm the correctness of the model.

The appropriateness of the carrier model, combined with our evidence that inosine is probably also a substrate for the transport system under study here (as discussed below), contradicts a suggestion by Quinlan and Hochstadt [25] that inosine transport into vesicles prepared from virus-transformed mouse 3T3 cells is a translocation process, involving the phosphorolysis of inosine to ribose 1-phosphate and hypoxanthine. This suggestion is based on the observation that the vesicles, after dilution in 0.8 M NaCl at 37°C and collection on nitrocellulose filters, contain no inosine or hypoxanthine, but an accumulation of ribose 1-phosphate derived from isotopically labeled inosine. The rapidity of nucleoside transport by carrier mediation suggests a different interpretation: inosine rapidly permeates the vesicles, intravesicular inosine is partially phosphoroylzed by residual phosphorylase, but it and product hypoxanthine exit during the filtration procedure, leaving only ribose 1-phosphate behind.

Although the mechanism of thymidine transport postulated here for cultured mammalian cells resembles in several respects that seen for nucleosides in human erythrocytes, it differs in respect to symmetry. In light of the studies of Cass and Paterson [26], Pickard and Paterson [27], and Cabantchik and Ginsburg [28] on uridine transport in erythrocytes (which, like the cells employed here, do not metabolize the transported substrate), we had anticipated asymmetries in the rate of movement of loaded and empty carrier. Based on graphical estimation of initial velocities of zero-*trans* entry and exit and of equilibrium exchange, Cabantchik and Ginsburg [28] reported V^{ee} for uridine

about 2.5-times V_{12}^{zt}. As we have not applied our sampling technology or integrated rate equations to erythrocytes, we are unable to judge whether the symmetry differences are real or artifactual.

The temperature studies (Figs. 5—7 and Table IV) also attest to the appropriateness of the symmetrical carrier model and extend it to a wide range of temperatures. Again, the conclusions based on a study of transport per se diverge from those based on a study of uptake [20]. In the latter case there was a distinct break in the Arrhenius curve of thymidine uptake (as for other nucleosides), which could be interpreted as indication of a phase transition in the membrane. Transport, as measured with zero-*trans* or equilibrium exchange protocol, did not show such a break. It is worth noting that the Arrhenius activation energy pertaining to transport at all temperatures (Fig. 6) is similar to that for uptake in the lower range of temperature [20]. The similarity suggests an alternative interpretation of the temperature discontinuity of uptake, namely a transition from permeation-limited uptake at low temperatures to kinase-limited uptake at high temperatures. The temperature dependence of thymidine transport makes also an important technical point: substantial amounts of free, intracellular nucleoside may be lost upon rinsing cells or vesicles even near ice temperature. For example, according to Fig. 5, a Novikoff cell would be expected to lose half its intracellular thymidine pool (if [thymidine] is less than, say, 100 μM) during a 43 s rinse with buffer at 4°C.

The inhibition of thymidine influx by several other nucleosides and bases (Fig. 8 and Table VI) we have taken as evidence of their all sharing a common transport system, a conclusion supported also by the fact that thymidine countertransports with a number of different nucleosides [10]. Moreover, a pattern of reciprocity of inhibition, at least among nucleosides, is becoming apparent in studies published [4,29] and in progress in this laboratory.

Still, we are unable to offer a quantitative interpretation of the inhibition data. It is not obvious why supposed alternate substrates for the thymidine transporter would elicit a change in V_{12}^{zt} as well as in K_{12}^{zt}, as is evident for all the inhibitors used in full kinetic analysis (Fig. 8).

The question of specificity is particularly troublesome in regard to nucleic acid base transport. By our criterion of inhibition, thymine, hypoxanthine and uracil would qualify as alternate substrates of the thymidine transporter in Novikoff cells, although of less affinity than nucleosides. (Cytosine did not inhibit thymidine transport, nor does it seem to be taken up by any saturable system, but rather by non-mediated permeation, as documented in Ref. 30.) Transport of hypoxanthine [31] and uracil [4] is mediated, but the reciprocity of inhibition we have seen among nucleosides does not seem strictly to apply between bases and nucleosides, suggesting the possibility that there may be also another transport system specific to bases.

But in spite the difficulties in interpreting inhibition data, a clear picture emerges from this study as a whole. Namely, thymidine is transported into mammalian cells by the simplest, carrier-mediated transport system imaginable. It does not require energy, but simply promotes the attainment of equilibrium distribution across the membrane. It is symmetrical in the sense that the carrier functions with equal facility whether loaded or empty, whether inbound or outbound. It operates independently of cellular metabolic machinery, nor is

itself a vectorial metabolic system. Its temperature dependence both with respect to transport velocity and carrier : substrate dissociation is unexceptional, with no abrupt changes indicative of phase transitions or the like. It seems relatively indiscriminate in regard to the substances it transports: a variety of natural artificial purine and pyrimidine ribosides and deoxyribosides appear to compete with thymidine, as, to a lesser extent, do some nucleic acid bases. And (to incorporate conclusions drawn elsewhere; Ref. 19) it is neither metabolically unstable nor subject to modulation with the growth stage of cultured cells.

If the thymidine (nucleoside) transport system is so simple, why has it been so elusive of characterization? The answer includes at least four interrelated parts. (i) The transport system is very fast (cf. Fig. 1). Rapid sampling techniques are essential to measure nucleoside flux. Moreover, even short rinses in substrate-free medium can eliminate such intracellular accumulation as has occurred. (ii) It is not very extensive, since substrate is not accumulated beyond its extracellular concentration. (iii) It is masked by intracellular metabolism. The intracellular accumulation of phosphorylated derivatives of exogenous, radiolabled nucleoside is extensive and prolonged compared to that of free nucleoside. The interference of metabolism is sufficient to mask the transport step even in vesicles largely devoid of cytoplasmic content [25]. (iv) Integrated rate equations for even the simplest carrier-mediated transport models are awkward enough to render their application an unattractive remedy for our inability to measure truly initial rates of substrate entry into cultured cells.

In light of the present and other recent results [1,3,4,7] and for the reasons enumerated above, it has become clear that the extensive literature on the kinetic characteristics of thymidine uptake in mammalian cells does not pertain to thymidine transport, and that the assessment of transport per se demands rapid sampling techniques and the use of non-metabolizable substrates.

Acknowledgements

The authors gratefully acknowledge expert technical assistance from John Erbe, Marsha Behrens, and Jill Myers, and the contributions of Cheryl Thull and Timothy Leonard to the preparation of the manuscript. Financial support for the work came from USPHS Research grant GM 24468, Training Grant CA 09138 (R.M.W. and R.M.), and Postdoctoral Fellowship CA 00800 (R.M.).

References

1 Wohlhueter, R.M., Marz, R., Graff, J.C. and Plagemann, P.G.W. (1976) J. Cell. Physiol. 89, 605—612
2 Wohlhueter, R.M., Marz, R., Graff, J.C. and Plagemann, P.G.W. (1978) in Methods in Cell Biology (Prescott, D., ed.), Vol. 20, pp. 211—236, Academic Press, New York
3 Marz, R., Wohlhueter, R.M. and Plagemann, P.G.W. (1977) J. Supramol. Struct. 6, 433—440
4 Plagemann, P.G.W., Marz, R. and Wohlhueter, R.M. (1978) J. Cell. Physiol. 97, 49—72
5 Eilam, Y. and Stein, W.D. (1974) in Methods in Membrane Biology (Korn, E.D., ed.), Vol. 2, pp. 283—354, Plenum Press, New York
6 Rozengurt, E., Stein, W.D. and Wigglesworth, N.M. (1977) Nature 267, 442—444
7 Koren, R., Shohami, E., Bibi, O. and Stein, W.D. (1978) FEBS Lett. 86, 71—75
8 Plagemann, P.G.W. and Swim, H.E. (1966) J. Bacteriol. 91, 2317—2326
9 Plagemann, P.G.W. (1976) J. Natl. Cancer Inst. 57, 1283—1295

10 Plagemann, P.G.W., Marz, R. and Erbe, J. (1976) J. Cell. Physiol. 89, 1—18
11 Kit, S., Dubbs, D.R., Piekarski, L.J. and Hsu, T.C. (1963) Exp. Cell Res. 31, 297—312
12 Wang, Y., Hogenkamp, H.P.C., Long, R.A., Revankar, G.R. and Robins, R.K. (1977) Carbohydr. Res. 59, 449—457
13 Plagemann, P.G.W. and Erbe, J. (1974) J. Cell. Physiol. 83, 321—336
14 Graff, J.C., Wohlhueter, R.M. and Plagemann, P.G.W. (1978) J. Cell. Physiol. 96, 171—188
15 Cleland, W.W. (1967) in Advances in Enzymology (Nord, F.F., ed.), Vol. 29, pp. 1—32, Interscience, New York
16 Pollard, J.H. (1977) A Handbook of Numerical and Statistical Techniques, pp. 275—299, Cambridge University Press, Cambridge
17 Dietrich, O.W. and Rothmann, O.S. (1975) Keyboard (Hewlett-Packard, Inc.) 7 (No. 4), 4—6
18 Wohlhueter, R.M., Marz, R. and Plagemann, P.G.W. (1978) J. Membrane Biol. 42, 247—264
19 Marz, R., Wohlhueter, R.M. and Plagemann, P.G.W. (1978) J. Supramol. Struct. 8, 511—520
20 Plagemann, P.G.W. and Erbe, J. (1975) J. Membrane Biol. 25, 381—396
21 Cleland, W.W. (1963) Biochim. Biophys. Acta 67, 173—187
22 Plagemann, P.G.W. and Richey, D.P. (1974) Biochim. Biophys. Acta 344, 263—305
23 Berlin, R.D. and Oliver, J.M. (1975) Int. Rev. Cytol. 42, 287—336
24 Oliver, J.M. and Paterson, A.R.P. (1971) Can. J. Biochem. 49, 262—270
25 Quinlan, D.C. and Hochstadt, J. (1976) J. Biol. Chem. 251, 344—354
26 Cass, C.E. and Paterson, A.R.P. (1972) J. Biol. Chem. 247, 3314—3320
27 Pickard, M.A. and Paterson, A.R.P. (1972) Can. J. Biochem. 50, 704—705
28 Cabantchik, Z.I. and Ginsburg, H. (1977) J. Gen. Physiol. 69, 75—96
29 Plagemann, P.G.W., Marz, R. and Wohlhueter, R.M. (1978) Cancer Res. 38, 978—989
30 Graff, J.C., Wohlhueter, R.M. and Plagemann, P.G.W. (1977) J. Biol. Chem. 252, 4185—4190
31 Marz, R., Wohlhueter, R.M. and Plagemann, P.G.W. (1979) J. Biol. Chem., in the press